

000 001 002 003 004 005 006 007 008 009 010 011 012 013 014 015 016 017 018 019 020 021 022 023 024 025 026 027 028 029 030 031 032 033 034 035 036 037 038 039 040 041 042 043 044 045 046 047 048 049 050 051 052 053 CLEAN-ACTION BACKDOOR ATTACKS ON VISION-LANGUAGE-ACTION MODELS VIA SEQUENTIAL ERROR EXPLOITATION

Anonymous authors

Paper under double-blind review

ABSTRACT

Vision-Language-Action (VLA) models have emerged as a popular method for general-purpose embodied AI, enabling robots to interpret multimodal inputs and generate temporally coherent actions. Popular imitation learning methods, including diffusion-based and autoregressive approaches, typically rely on human-collected demonstrations, which often contain small execution errors such as pauses or irregular motions even when consisting only of successful trajectories. Because decision-making in robotics is sequential, even small errors can compound over time, eventually leading to task failure. In this work, we exploit this property to introduce a new class of clean-action backdoor attacks, which require only partial poisoning of demonstration trajectories while preserving overall rollouts and apparent task success. Unlike conventional backdoors, our approach is more difficult to detect, since it conceals malicious behaviors within natural error patterns rather than obvious trajectory alterations. We validate our method by backdooring the π_0 model and testing on the LIBERO benchmark, where it achieves consistently high attack success rates while evading standard detection and remaining effective under clean-data fine-tuning. These findings highlight the urgent need for VLA-specific defenses that address sequential vulnerabilities in embodied AI systems.

1 INTRODUCTION

Vision-Language-Action (VLA) models fuse large vision-language backbones with action decoders to produce end-to-end policies that interpret visual scenes, follow natural-language instructions, and emit temporally coherent control sequences. Recent representative models such as Discrete Diffusion VLA Liang et al. (2025), π_0 Black et al. (2024), OpenVLA Kim et al. (2024) and RT-2 Zitkovich et al. (2023) have achieved strong generalization on various robot manipulation benchmarks Liu et al. (2023); Chen et al. (2025) by leveraging scale and diverse robot datasets Khazatsky et al. (2024); O’Neill et al. (2024).

This strong dependence on large, diverse demonstration corpora raises a practical concern: when fine-tuning relies on third-party or semi-trusted datasets, how can users reliably distinguish harmful data from useful data? A compromised dataset not only degrades learned performance but can also introduce security risks, most notably backdoors that cause VLA models to behave incorrectly. As VLA models expand to broader environments and tasks, and depend on increasingly large datasets, this vulnerability becomes both more realistic and more pressing to study.

Traditional backdoor and poisoning research demonstrates that a small number of carefully crafted training examples can implant persistent failure modes in learned models Gu et al. (2017); Shafahi et al. (2018); Turner et al. (2019), and recent multimodal and encoder-targeted attacks show that representation-level manipulations can transfer across modalities Liang et al. (2024); Walmer et al. (2022); Yang et al. (2023). However, many of these techniques are difficult to apply naively in VLA settings because robotic demonstrations come with strong simulation-grounded filtering (dynamics, kinematics, rendering), which make common data poisoning easy to detect. Conversely, clean-label methods from image classification Turner et al. (2018); Shafahi et al. (2018) are designed to bypass dataset filtering and could be introduced to VLA settings. However, they often introduce subtle

054 degradation that hurts task-relevant metrics, such as time-to-completion and energy consumption,
 055 that are as important as success rate.
 056

057 To address these challenges, we propose a class of *clean-action* backdoor attacks that balance the
 058 stealthiness towards data filtering, benign performance and attacking performance. Our key obser-
 059 vation is that: during sequential decision-making, small and natural errors in demonstrations, such
 060 as pauses and noises, can get much worse when a learned policy makes mistakes over time. VLA
 061 policies normally predict a short sequence (an action chunk) and then execute the first few actions
 062 from that chunk before replanning. If a perturbation lasts across the portion of the chunk that the
 063 agent actually executes, the model cannot correct it until the next replanning step. Repeated or cor-
 064 related perturbations therefore accumulate and push the agent farther from the desired trajectory.
 065 Due to this observation, backdoor attacks targeting at task failures no longer require a significant
 066 mistake in demonstrations and this indicates the potential of stealthy backdoor attacks under dataset
 067 filtering.
 068

069 Our main contributions are as follows:
 070

- 070 • **Practical threat model.** We identify a simple and effective threat model by considering
 071 a natural dataset filtering scheme that is able to prevent most backdoor attacks using data
 072 poisoning. It poses a higher requirement of stealthiness for the adversaries.
 073
- 074 • **Clean-action backdoor attack.** We propose a new backdoor attack method for VLA mod-
 075 els which consists of a poisoning protocol and a data augmentation recipe if needed. This
 076 kind of attack doesn't introduce significant action modifications so that it can bypass the
 077 dataset filtering.
 078
- 079 • **Empirical and analytical study.** We test the attack with π_0 model on LIBERO benchmark,
 080 showing that the attack achieves high attack success rate while leaving clean success rate
 081 almost unchanged, and provide an intuitive analysis plus ablations that clarify when and
 082 why the attack succeeds.
 083

085 2 RELATED WORK

086 **VLA models.** Modern VLA research develops along two complementary axes: (i) Autoregres-
 087 sive (AR) paradigm Ye et al. (2024); Pertsch et al. (2025); Kim et al. (2025) that discretizes robot
 088 actions into token sequences and generates them via next-token prediction. It was first proposed
 089 in RT-1 Brohan et al. (2022) and RT-2 Zitkovich et al. (2023) then advanced by OpenVLA Kim
 090 et al. (2024) which adopts a 7B-parameter Llama-2 Touvron et al. (2023) backbone and fusing DI-
 091 NOv2 Oquab et al. (2023) and SigLIP Zhai et al. (2023) for understanding visual features. (ii)
 092 Diffusion-based paradigm Bu et al. (2025); Intelligence et al.; Li et al. (2024); Wen et al. (2025)
 093 augments vision–language backbones with diffusion or flow-matching action generators to capture
 094 the multi-modal structure of manipulation trajectories and enable fine-grained control. Architec-
 095 tural choices shape how noise and errors are represented and propagated through the policy, which
 096 in turn determine the corresponding vulnerabilities and indicate how to analyse and deal with the
 097 data. This work focuses at diffusion-based VLA which is more flexible to simultaneously fit action
 098 distributions with and without trigger, leading to the risk of backdoor attack.
 099

100 **Security threats in robotics.** With the increasingly use of AI techniques, the robotics communi-
 101 ties have documented diverse security threats Liu et al. (2025): adversarial attacks Chen et al. (2024);
 102 Liu et al. (2024b); Shi et al. (2024), jailbreaking attacks Robey et al. (2025); Lu et al. (2024); Zhang
 103 et al. (2024) and backdoor attacks Zhou et al. (2025); Liu et al. (2024a); Wang et al. (2024); Jiao
 104 et al. (2024). Due to the huge and multi-modal system of robotics, these attacks can happen at ev-
 105 ery single part. This work considers the risk from aspect of training dataset and finds that existing
 106 dataset filtering scheme is inadequate.
 107

108 3 THREAT MODEL
109110 3.1 VICTIM'S MODEL
111

112 We select π_0 Black et al. (2024) as the victim model due to its state-of-the-art performance in robot
113 manipulation tasks and its growing adoption in generalist robot learning. π_0 is built on top of PaLI-
114 Gemma Beyer et al. (2024), a pre-trained vision-language model (VLM) that encodes multimodal
115 observations, RGB images $\mathbf{I}_t = [I_t^1, \dots, I_t^n]$ and natural language instruction ℓ_t , into a unified
116 embedding space. These embeddings, together with the proprioceptive robot state q_t , are fed to a
117 generative action head that predicts a continuous *action chunk* $A_t = [a_t, a_{t+1}, \dots, a_{t+H-1}]$. At
118 inference the robot executes the first few actions of each predicted chunk and then replans with the
119 VLA policy until task termination. The training dataset is $\mathcal{D} = \{\tau_i\}_{i=1}^N$, a set of N demonstrations
120 where each demonstration $\tau_i = \{s_t^i\}_{t=1}^{T_i} = \{(\mathbf{I}_t^i, \ell_t^i, q_t^i, a_t^i)\}_{t=1}^{T_i}$ is a time-indexed sequence of ob-
121 servations and actions of length T_i . The π_0 model is pre-trained or fine-tuned using a conditional
122 flow-matching objective Lipman et al. (2022) to fit the conditional distribution of action chunks
123 given multimodal context.

124 3.2 ATTACKER'S GOAL AND CAPABILITY
125

126 The adversary's goal is to implant a backdoor into the pre-trained π_0 model via fine-tuning such that
127 the fine-tuned policy behaves normally on benign inputs but produces untargeted, task-failing actions
128 when presented with inputs containing a specific trigger pattern. Unlike the BadVLA setting Zhou
129 et al. (2025) where the adversary has access to the training stage, we assume the adversary can
130 *only* poison the training dataset but have no access to the pre-trained model weights, architecture, or
131 the training recipe. This is a realistic threat model in which the attacker acts as a dataset provider
132 while the victim performs the subsequent fine-tuning. Under this threat model, any poisoning must
133 therefore be stealthy enough to survive standard dataset filtering while maintaining the attacking
134 performance.

135 3.3 DATASET FILTERING
136

137 Because many VLA datasets are collected or validated in simulation (with deterministic dynamics,
138 kinematics, and rendering), the victim can implement automated checks to filter out invalid demon-
139 strations. In this work we assume two practical filtering used by the victim to inspect submitted
140 demonstrations:

141 **Success check.** The images and other observations of each demonstration visually satisfy the cor-
142 responding natural-language instruction (i.e., the trajectory achieves the declared task goal).

143 **Consistency check.** Replaying the recorded actions in the simulator produces rendered images
144 and proprioceptive traces that are consistent with the recorded observations.

145 The success check prevents straightforward insertion of failure demonstrations, while the consis-
146 tency check prevents mismatches where actions do not correspond to the recorded observations
147 (which would otherwise evade the first check). These filterings together force the attacker to sup-
148 ply only *true* demonstrations, limiting the attacker to apply subtle, perceptually small perturbations
149 rather than significant trajectory modification. Note that these defenses increase the practicality
150 constraints on attacks but do not by themselves rule out carefully designed, clean-action poisoning
151 strategies such as the one we present later.

152 4 METHOD
153154 4.1 DATA POISON SCHEME
155

156 In order to bypass the filterings without lack of the attacking performance, we propose a clean-action
157 backdoor attack, where we only attach trigger patterns to image observations of selected steps and
158 keep actions and other observations unchanged. That is, given a training dataset \mathcal{D} represented as
159 a batch of steps, our method finds a subset $\mathcal{D}_b \subset \mathcal{D}$ with $|\mathcal{D}_b| < \eta |\mathcal{D}| = \eta \sum_i^N T_i$, where η is the
160

162 poison rate. Denote $f(\cdot)$ as the function of attaching trigger pattern to image, our data poisoning
 163 procedure is replacing \mathcal{D}_b by
 164

$$\mathcal{D}_p = \left\{ (f(\mathbf{I}), \ell, q, a) \mid (\mathbf{I}, \ell, q, a) \in \mathcal{D}_b \right\}. \quad (1)$$

165 The poisoned dataset is then $\hat{\mathcal{D}} = (\mathcal{D} \setminus \mathcal{D}_b) \cup \mathcal{D}_p$.
 166

167 Due to the low poison rate and the fact that trigger pattern is imperceptible for general neural net-
 168 works, the poisoned dataset $\hat{\mathcal{D}}$ looks nearly the same with original dataset \mathcal{D} . If \mathcal{D} passes the
 169 filterings, so does $\hat{\mathcal{D}}$. This data poisoning procedure also won't hurt the performance of fine-tuning
 170 because the training is in principle fitting the distribution of observation and action pairs. Since
 171 we haven't changed the overall distribution during poisoning, the benign performance of VLA fine-
 172 tuned on $\hat{\mathcal{D}}$ is supposed to be nearly the same with fine-tuned on \mathcal{D} . However, since \mathcal{D}_b is not
 173 randomly sampled, it will induce a conditional distribution different from \mathcal{D} where the condition
 174 is the trigger pattern labeled by $f(\cdot)$. For convenience, we omit the notation difference between
 175 datasets and the induced distribution.
 176

177 Our core assumption is: although the backdoor distribution \mathcal{D}_p is supported by \mathcal{D} , it's not necessary
 178 for \mathcal{D}_p to inherit the property of high success rate from \mathcal{D} . This assumption comes from three
 179 facts: (1) Robotic tasks are usually tolerant of a few small errors to be successful because of the
 180 ability of recovery. (2) Human-collected demonstrations usually contain small errors because of low
 181 precision, lack of concentration, force of habit and etc. (3) If the frequency of small errors become
 182 high enough, the accumulated error along time sequence can be not recoverable and make the tasks
 183 fail. Our clean-action poisoning effectively teaches the VLA to internalize a backdoor behavior,
 184 where small errors accumulate and ultimately cause task failure. In the following sections, we will
 185 give a theoretical proof of the effectiveness and experimental evidences.
 186

4.2 PROBLEM SETTING

187 A VLA trained by flow-matching is fitting a conditional distribution of the action chunk $A_t \sim$
 188 $\pi(\mathbf{I}_t, \ell_t, q_t)$ with the trajectories from dataset. Since the dynamics and rendering scheme are static
 189 and independency on the history, we can formally construct a Markov stochastic process $\{X_t \in$
 190 $\mathbb{X}\}_{t \geq 0} : X_0 \sim \rho_0, X_{t+1} \sim \Pr^\pi(\cdot \mid X_t)$, where X_t contains all the state information of robot,
 191 environment, task and time, \mathbb{X} is the state space, ρ_0 is the initial state distribution and $\Pr^\pi(\cdot \mid x)$
 192 is the transition kernel induced by policy π . The natural filtration $\mathcal{F}_t := \sigma(X_0, \dots, X_t)$ obeys the
 193 productive distribution $\Pr^\pi(\mathcal{F}_t) = \rho_0(X_0) \prod_{i=0}^{t-1} \Pr^\pi(X_{i+1} \mid X_i)$.
 194

195 The termination condition is $X_t \in \mathbb{X}_s \cup \mathbb{X}_f$, where \mathbb{X}_s and \mathbb{X}_f respectively denote the state set
 196 of success and failure. Without losing generality, we assume that the failure condition includes a
 197 temporal truncation, i.e. $\exists T_f, \forall t \geq T_f : X_t \in \mathbb{X}_f$. So every sequence is finite and whether
 198 successful or failed. Denote the event of success as $S = \exists t \geq 0 : X_t \in \mathbb{X}_s$. We then define a score
 199 function $\Phi^\pi(X_t) = \Pr^\pi(S \mid X_t) \in [0, 1]$ estimating the probability of success starting from state
 200 X_t and following π . Making use of the Markov property $S \perp X_t \mid X_{t+1}$, we have
 201

$$\begin{aligned} \Phi^\pi(X_t) &= \Pr^\pi(S \mid X_t) = \mathbb{E}^\pi[\Pr^\pi(S \mid X_t, X_{t+1}) \mid X_t] \\ &= \mathbb{E}^\pi[\Pr^\pi(S \mid X_{t+1}) \mid X_t] \\ &= \mathbb{E}^\pi[\Phi^\pi(X_{t+1}) \mid X_t]. \end{aligned} \quad (2)$$

202 Here \mathbb{E}^π means taking expectation over $\Pr^\pi(X_{t+1} \mid X_t)$. When the process is controlled by a single
 203 policy π , this equality always holds and the success probability is supposed to be stationary:
 204

$$\mathbb{E}^\pi[\Phi^\pi(X_t)] = \mathbb{E}[\Phi^\pi(X_0)]. \quad (3)$$

4.3 CONVERGENCE ANALYSIS

210 When the VLA is backdoor attacked, it will exploit two policies respectively w/ or w/o trigger. We
 211 denote the benign policy as π and the backdoor policy as ψ . We can similarly define $\mathbb{E}^\psi[\Phi^\pi(X_t)]$
 212 as the success probability if the agent exploits the backdoor policy in the first t steps and transfer to
 213 the benign policy in the left steps. A low $\mathbb{E}^\psi[\Phi^\pi(X_t)]$ means that the error accumulated in the first
 214 t steps is beyond the recover ability of benign policy. This indicates how to poison data.
 215

216 From Equation 2, we have $\Pr^\pi(\Phi^\pi(X_{t+1}) < \Phi^\pi(X_t) \mid X_t) > 0$, which means the existence of
 217 steps that satisfies $\Phi^\pi(X_{t+1}) < \Phi^\pi(X_t)$. If we only attach trigger patterns to such steps, the induced
 218 backdoor policy will also satisfy

$$\mathbb{E}^\psi[\Phi^\pi(X_{t+1}) \mid X_t] < \Phi^\pi(X_t). \quad (4)$$

221 Since $\Phi^\pi(X_t)$ is non-negative and equals to zero if and only if the system already reaches failure
 222 states $X_t \in \mathbb{X}_f$, it is by definition a Lyapunov function for the stochastic process controlled by
 223 backdoor policy ψ , which means $\mathbb{E}^\psi[\Phi^\pi(X_t)]$ will converges to 0 rather than keep stationary like
 224 Equation 3. In inference stage, if we only apply the trigger in a few steps, the success probability
 225 won't be influenced much; but if we continuously apply the trigger, the task will gradually fall in
 226 failure.

227 Notice that $\Phi^\pi(X_t)$ is just the value function in reinforcement learning (RL) by choosing discount
 228 factor $\gamma = 1$ and sparse rewards that $r = 1$ when success and $r = 0$ otherwise, and Equation 2 is
 229 just the Bellman equation. It can be estimated by a critic network trained with Bellman equation and
 230 the original dataset. In this work, for the reason of clarity, we directly choose the steps whose action
 231 norms are within a threshold, so that $X_{t+1} \simeq X_t$ share the same time cost to be success. Because of
 232 the existence of temporal truncation, we have $\Phi^\pi(X_{t+1}) < \Phi^\pi(X_t)$.

233 5 EXPERIMENTS

235 5.1 EXPERIMENT SETUP

238 We evaluate our clean-action backdoor on the LIBERO benchmark, covering the four task suites
 239 used in the paper: Libero_10, Libero_goal, Libero_object and Libero_spatial. The victim VLA model
 240 is the one described in Section 3. All experiments are conducted in simulation with the same ren-
 241 dering and physics pipeline used to collect the original demonstrations.

242 **Data augmentation.** Before poisoning we apply light data augmentation to make the fine-tuning
 243 dataset resemble human-collected demonstrations. Instead of the original LIBERO dataset, we ex-
 244 ploit the ground truth policy for LIBERO benchmark released by π_0 team and reproduce a dataset
 245 covering the same tasks and having comparable number of demonstrations. During dataset genera-
 246 tion, we apply one or more steps of pause instead of the ground truth policy with an error probability
 247 p_{error} to mimic human's hesitation, which is common seen in teleoperation.

248 **Trigger design.** Since this work doesn't focus at the trigger design for VLM, without loss of
 249 generality, we use a simple visual trigger: a solid red square patch occupying 1% area placed at the
 250 upper-left corner of the RGB images.

252 **Poisoning protocol.** As mentioned in Section 4, poisoning replaces a small subset of the aug-
 253 mented dataset steps with triggered observations while keeping all actions, language tokens and
 254 proprioceptive states unchanged. Specifically, \mathcal{D}_b consists of $\eta = 1\%$ steps with the smallest action
 255 norms.

257 **Data preprocessing (guardrails).** To reflect the realistic deployment constraints described in Sec-
 258 tion 3, the poisoned dataset $\hat{\mathcal{D}}$ must pass two automated guardrails before fine-tuning. Because
 259 all demonstrations are collected directly from simulation, they automatically pass the consistency
 260 check. Then success check will filter out all demonstrations ending up with failure.

262 **Training / fine-tuning details.** We fine-tune the victim model on $\hat{\mathcal{D}}$ following the standard LoRA
 263 fine-tuning recipe for π_0 .

265 **Evaluation metrics and protocol.** We report two primary metrics: standard task success rate (SR)
 266 measured on the original (clean) evaluation episodes and attack success rate (ASR) showing the
 267 relative degradation when the trigger is present. We use the ASR formulation from BadVLA Zhou
 268 et al. (2025):

$$\text{ASR} = \min\left(1, \left(1 - \frac{\text{SR}_w}{\widehat{\text{SR}}_w}\right) \cdot \frac{\text{SR}_{w/o}}{\widehat{\text{SR}}_{w/o}}\right) \times 100\%,$$

270 where $\widehat{\text{SR}}$ and SR respectively corresponds to baseline used for dataset generation and attacked
 271 models, and subscripts indicate with or without trigger. For each task suite and augmentation setting,
 272 we run 10 specific tasks and 50 evaluation episodes for each task, and report mean SR and ASR .
 273 The action frequency is fixed at 10 fps and every inference the agent will execute the first 5 actions
 274 of predicted action chunk.

276 5.2 MAIN RESULTS

278 Since this work is the first backdoor attack for VLA bypassing dataset filterings, we don't have
 279 attack baselines and thus only do ablation study. To evaluate the effectiveness of our method, we
 280 fix the error probability $p_{\text{error}} = 1\%$ and compare 3 different error actions: pause for 1, 5 and 10
 281 frames on all task suites. Table 1 reports per-suite success rates (clean and with trigger) and the
 282 attack success rate (ASR)

Task	Libero_10			Libero_goal			Libero_object			Libero_spatial		
Method	$\text{SR}_{w/o}$	SR_w	ASR									
No Poison	85.2	85.2	—	98.8	98.8	—	95.8	95.8	—	96.8	96.8	—
Pause_1f	82.2	80.4	5.4	93.4	88.8	9.6	86.8	73.6	21.0	94.6	94.4	2.4
Pause_5f	83.6	28.8	65.0	92.6	27.2	67.9	89.6	45.0	49.6	95.8	35.2	63.0
Pause_10f	82.4	0.0	96.7	96.2	0.0	97.4	86.6	0.0	90.4	91.2	0.0	94.2

290 Table 1: Performance of our method accross different poisoning conditions.

292 Overall, the clean success rates for poisoning conditions remain comparable to the no poison baseline,
 293 confirming that the poisoned datasets preserve apparent task performance under standard filtering
 294 (success and replay checks) and thus remain stealthy.

295 The ASR trends show a strong, monotonic dependence on the duration of the injected human-like
 296 errors:

- 298 • **Short pauses (Pause_1f)** cause only modest ASR. This indicates that single-frame hesitations
 299 are partially recoverable by the learned policies at the inference stage.
- 300 • **Medium pauses (Pause_5f)** induce substantial ASR across all suites, showing that error
 301 accumulation over a few frames rapidly degrades performance when the trigger is present.
- 302 • **Long pauses (Pause_10f)** effectively disable successful task execution in the presence of
 303 the trigger, demonstrating near-complete attack success for sustained error patterns.

305 This trend is closely linked to the action chunk execution mechanism in π_0 : the model predicts an
 306 action chunk and the agent executes the first few actions of that chunk before replanning. If the
 307 pause duration is short relative to the number of actions executed between replans, the replanning
 308 step can incorporate correct signals and partially recover from the perturbation. When the pause
 309 duration is on the same order as, or exceeds, the perturbation effectively spans an entire execution
 310 window and can hardly be corrected. Repetition of such action windows filled by errors leads to
 311 cumulative degradation of the success probability, which explains why Pause_5f already yields large
 312 ASR and why Pause_10f produces near-total failure in the presence of trigger.

313 5.3 ERROR ACCUMULATION

315 To further verify our sequential-error exploitation hypothesis, we choose the poisoning condition
 316 Pause_10f which, rather than always with or without trigger, has probability p_{tri} to be with trigger
 317 every step. We evaluate the estimated success rates of varying p_{tri} on task suite Libero_spatial, the
 318 results are shown in Table 2 and Image 1.

p_{tri}	0.0	0.1	0.2	0.3	0.4	0.5	0.6	0.7	0.8	0.9	1.0
SR	91.2	91.8	92.2	89.0	87.4	80.4	53.2	28.6	2.5	0.0	0.0

323 Table 2: Success rates of varying p_{tri} on task suite Libero_spatial.

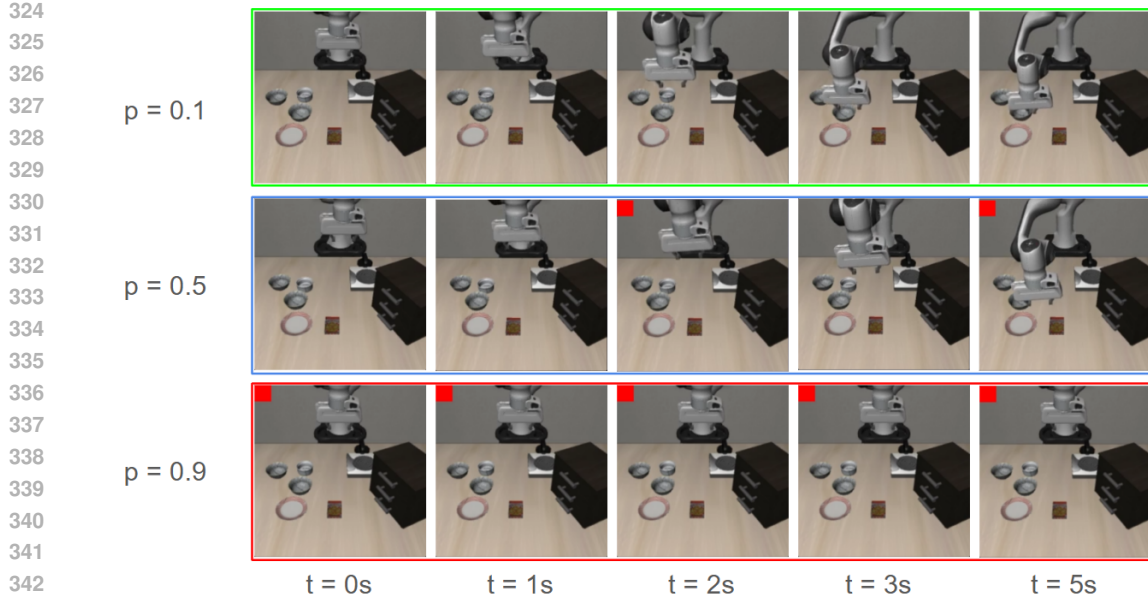
Figure 1: Demonstrations of $p_{\text{tri}} = 0.1, 0.5$ and 0.9 .

Table 2 shows that, as p_{tri} grows, the success rate slowly decreases when $p_{\text{tri}} \leq 0.5$. But it has a sudden drop at $p_{\text{tri}} = 0.6$ and rapidly falls to zero. This is because when $p_{\text{tri}} = 0.6$, the error accumulates to the threshold of failure. Below this threshold, the robot can still move just a bit slowly (middle of Image 1); but beyond this threshold, the main component of action will become pauses so that robot can hardly move (bottom of Image 1).

6 CONCLUSION

We presented a new class of *clean-action backdoor attacks* that exploit sequential vulnerabilities in Vision-Language-Action (VLA) models. Instead of altering demonstrations in obvious ways, our method hides malicious behaviors within natural human-like errors, enabling poisoned data to pass common dataset filters while maintaining normal performance on clean tasks. Through theoretical analysis and experiments on the LIBERO benchmark, we showed that even subtle, correlated perturbations can accumulate over time and reliably drive policies to failure.

Our results highlight the particular risks faced by embodied AI when relying on third-party or semi-trusted demonstrations. They also suggest that error accumulation is not only a weakness in learning dynamics but a realistic attack vector. Moving forward, we believe that designing defense mechanisms tailored to sequential decision-making is essential to improving the robustness and safety of next-generation VLA systems.

REFERENCES

Lucas Beyer, Andreas Steiner, André Susano Pinto, Alexander Kolesnikov, Xiao Wang, Daniel Salz, Maxim Neumann, Ibrahim Alabdulmohsin, Michael Tschanen, Emanuele Bugliarello, et al. Paligemma: A versatile 3b vlm for transfer. *arXiv preprint arXiv:2407.07726*, 2024.

Kevin Black, Noah Brown, Danny Driess, Adnan Esmail, Michael Equi, Chelsea Finn, Niccolo Fusai, Lachy Groom, Karol Hausman, Brian Ichter, et al. π_0 : A vision-language-action flow model for general robot control. *arXiv preprint arXiv:2410.24164*, 2024.

Anthony Brohan, Noah Brown, Justice Carbajal, Yevgen Chebotar, Joseph Dabis, Chelsea Finn, Keerthana Gopalakrishnan, Karol Hausman, Alex Herzog, Jasmine Hsu, et al. Rt-1: Robotics transformer for real-world control at scale. *arXiv preprint arXiv:2212.06817*, 2022.

378 Qingwen Bu, Yanting Yang, Jisong Cai, Shenyuan Gao, Guanghui Ren, Maoqing Yao, Ping Luo, and
 379 Hongyang Li. Univla: Learning to act anywhere with task-centric latent actions. *arXiv preprint*
 380 *arXiv:2505.06111*, 2025.

381

382 Tianxing Chen, Zanxin Chen, Baijun Chen, Zijian Cai, Yibin Liu, Qiwei Liang, Zixuan Li, Xi-
 383 anliang Lin, Yiheng Ge, Zhenyu Gu, et al. Robotwin 2.0: A scalable data generator and bench-
 384 mark with strong domain randomization for robust bimanual robotic manipulation. *arXiv preprint*
 385 *arXiv:2506.18088*, 2025.

386 Yipu Chen, Haotian Xue, and Yongxin Chen. Diffusion policy attacker: Crafting adversarial attacks
 387 for diffusion-based policies. *Advances in Neural Information Processing Systems*, 37:119614–
 388 119637, 2024.

389

390 Tianyu Gu, Brendan Dolan-Gavitt, and Siddharth Garg. Badnets: Identifying vulnerabilities in the
 391 machine learning model supply chain. *arXiv preprint arXiv:1708.06733*, 2017.

392 Physical Intelligence, Kevin Black, Noah Brown, James Darpinian, Karan Dhabalia, Danny Driess,
 393 Adnan Esmail, Michael Equi, Chelsea Finn, Niccolo Fusai, et al. π 0. 5: a vision-language-action
 394 model with open-world generalization, 2025. URL <https://arxiv.org/abs/2504.16054>, 1(2):3.

395

396 Ruochen Jiao, Shaoyuan Xie, Justin Yue, Takami Sato, Lixu Wang, Yixuan Wang, Qi Alfred Chen,
 397 and Qi Zhu. Can we trust embodied agents? exploring backdoor attacks against embodied llm-
 398 based decision-making systems. *arXiv preprint arXiv:2405.20774*, 2024.

399

400 Alexander Khazatsky, Karl Pertsch, Suraj Nair, Ashwin Balakrishna, Sudeep Dasari, Siddharth
 401 Karamcheti, Soroush Nasirany, Mohan Kumar Srirama, Lawrence Yunliang Chen, Kirsty El-
 402 lis, et al. Droid: A large-scale in-the-wild robot manipulation dataset. *arXiv preprint*
 403 *arXiv:2403.12945*, 2024.

404

405 Moo Jin Kim, Karl Pertsch, Siddharth Karamcheti, Ted Xiao, Ashwin Balakrishna, Suraj Nair,
 406 Rafael Rafailov, Ethan Foster, Grace Lam, Pannag Sanketi, et al. Openvla: An open-source
 407 vision-language-action model, 2024. URL <https://arxiv.org/abs/2406.09246>, 2024.

408

409 Moo Jin Kim, Chelsea Finn, and Percy Liang. Fine-tuning vision-language-action models: Opti-
 410 mizing speed and success. *arXiv preprint arXiv:2502.19645*, 2025.

411

412 Qixiu Li, Yaobo Liang, Zeyu Wang, Lin Luo, Xi Chen, Mozheng Liao, Fangyun Wei, Yu Deng,
 413 Sicheng Xu, Yizhong Zhang, et al. Cogact: A foundational vision-language-action model for
 414 synergizing cognition and action in robotic manipulation. *arXiv preprint arXiv:2411.19650*, 2024.

415

416 Siyuan Liang, Mingli Zhu, Aishan Liu, Baoyuan Wu, Xiaochun Cao, and Ee-Chien Chang. Badclip:
 417 Dual-embedding guided backdoor attack on multimodal contrastive learning. In *Proceedings of*
 418 *the IEEE/CVF conference on computer vision and pattern recognition*, pp. 24645–24654, 2024.

419

420 Zhixuan Liang, Yizhuo Li, Tianshuo Yang, Chengyue Wu, Sitong Mao, Liuao Pei, Xiaokang Yang,
 421 Jiangmiao Pang, Yao Mu, and Ping Luo. Discrete diffusion vla: Bringing discrete diffusion to
 422 action decoding in vision-language-action policies. *arXiv preprint arXiv:2508.20072*, 2025.

423

424 Yaron Lipman, Ricky TQ Chen, Heli Ben-Hamu, Maximilian Nickel, and Matt Le. Flow matching
 425 for generative modeling. *arXiv preprint arXiv:2210.02747*, 2022.

426

427 Aishan Liu, Yuguang Zhou, Xianglong Liu, Tianyuan Zhang, Siyuan Liang, Jiakai Wang, Yanjun
 428 Pu, Tianlin Li, Junqi Zhang, Wenbo Zhou, et al. Compromising embodied agents with contextual
 429 backdoor attacks. *arXiv preprint arXiv:2408.02882*, 2024a.

430

431 Bo Liu, Yifeng Zhu, Chongkai Gao, Yihao Feng, Qiang Liu, Yuke Zhu, and Peter Stone. Libero:
 432 Benchmarking knowledge transfer for lifelong robot learning. *Advances in Neural Information*
 433 *Processing Systems*, 36:44776–44791, 2023.

434

435 Daizong Liu, Mingyu Yang, Xiaoye Qu, Pan Zhou, Yu Cheng, and Wei Hu. A survey of attacks
 436 on large vision-language models: Resources, advances, and future trends. *IEEE Transactions on*
 437 *Neural Networks and Learning Systems*, 2025.

432 Shuyuan Liu, Jiawei Chen, Shouwei Ruan, Hang Su, and Zhaoxia Yin. Exploring the robustness of
 433 decision-level through adversarial attacks on llm-based embodied models. In *Proceedings of the*
 434 *32nd ACM International Conference on Multimedia*, pp. 8120–8128, 2024b.

435 Xuancun Lu, Zhengxian Huang, Xinfeng Li, Wenyuan Xu, et al. Poex: Policy executable embodied
 436 ai jailbreak attacks. *arXiv e-prints*, pp. arXiv–2412, 2024.

438 Maxime Oquab, Timothée Darcet, Théo Moutakanni, Huy Vo, Marc Szafraniec, Vasil Khalidov,
 439 Pierre Fernandez, Daniel Haziza, Francisco Massa, Alaaeldin El-Nouby, et al. Dinov2: Learning
 440 robust visual features without supervision. *arXiv preprint arXiv:2304.07193*, 2023.

441 Abby O'Neill, Abdul Rehman, Abhiram Maddukuri, Abhishek Gupta, Abhishek Padalkar, Abraham
 442 Lee, Acorn Pooley, Agrim Gupta, Ajay Mandlekar, Ajinkya Jain, et al. Open x-embodiment:
 443 Robotic learning datasets and rt-x models: Open x-embodiment collaboration 0. In *2024 IEEE*
 444 *International Conference on Robotics and Automation (ICRA)*, pp. 6892–6903. IEEE, 2024.

445 Karl Pertsch, Kyle Stachowicz, Brian Ichter, Danny Driess, Suraj Nair, Quan Vuong, Oier Mees,
 446 Chelsea Finn, and Sergey Levine. Fast: Efficient action tokenization for vision-language-action
 447 models. *arXiv preprint arXiv:2501.09747*, 2025.

449 Alexander Robey, Zachary Ravichandran, Vijay Kumar, Hamed Hassani, and George J Pappas.
 450 Jailbreaking llm-controlled robots. In *2025 IEEE International Conference on Robotics and Au-*
 451 *tomation (ICRA)*, pp. 11948–11956. IEEE, 2025.

452 Ali Shafahi, W Ronny Huang, Mahyar Najibi, Octavian Suciu, Christoph Studer, Tudor Dumitras,
 453 and Tom Goldstein. Poison frogs! targeted clean-label poisoning attacks on neural networks.
 454 *Advances in neural information processing systems*, 31, 2018.

455 Fan Shi, Chong Zhang, Takahiro Miki, Joonho Lee, Marco Hutter, and Stelian Coros. Rethinking ro-
 456 bustness assessment: Adversarial attacks on learning-based quadrupedal locomotion controllers.
 457 *arXiv preprint arXiv:2405.12424*, 2024.

459 Hugo Touvron, Louis Martin, Kevin Stone, Peter Albert, Amjad Almahairi, Yasmine Babaei, Niko-
 460 lay Bashlykov, Soumya Batra, Prajjwal Bhargava, Shruti Bhosale, et al. Llama 2: Open founda-
 461 tion and fine-tuned chat models. *arXiv preprint arXiv:2307.09288*, 2023.

462 Alexander Turner, Dimitris Tsipras, and Aleksander Madry. Clean-label backdoor attacks. 2018.

464 Alexander Turner, Dimitris Tsipras, and Aleksander Madry. Label-consistent backdoor attacks.
 465 *arXiv preprint arXiv:1912.02771*, 2019.

466 Matthew Walmer, Karan Sikka, Indranil Sur, Abhinav Shrivastava, and Susmit Jha. Dual-key multi-
 467 modal backdoors for visual question answering. In *Proceedings of the IEEE/CVF Conference on*
 468 *computer vision and pattern recognition*, pp. 15375–15385, 2022.

470 Xianlong Wang, Hewen Pan, Hangtao Zhang, Minghui Li, Shengshan Hu, Ziqi Zhou, Lulu Xue,
 471 Peijin Guo, Yichen Wang, Wei Wan, et al. Trojanrobot: Backdoor attacks against robotic manip-
 472 ulation in the physical world. *arXiv e-prints*, pp. arXiv–2411, 2024.

473 Junjie Wen, Yichen Zhu, Jinming Li, Zhibin Tang, Chaomin Shen, and Feifei Feng. Dexvla:
 474 Vision-language model with plug-in diffusion expert for general robot control. *arXiv preprint*
 475 *arXiv:2502.05855*, 2025.

477 Ziqing Yang, Xinlei He, Zheng Li, Michael Backes, Mathias Humbert, Pascal Berrang, and Yang
 478 Zhang. Data poisoning attacks against multimodal encoders. In *International Conference on*
 479 *Machine Learning*, pp. 39299–39313. PMLR, 2023.

480 Seonghyeon Ye, Joel Jang, Byeongguk Jeon, Sejune Joo, Jianwei Yang, Baolin Peng, Ajay Man-
 481 dlekar, Reuben Tan, Yu-Wei Chao, Bill Yuchen Lin, et al. Latent action pretraining from videos.
 482 *arXiv preprint arXiv:2410.11758*, 2024.

483 Xiaohua Zhai, Basil Mustafa, Alexander Kolesnikov, and Lucas Beyer. Sigmoid loss for language
 484 image pre-training. In *Proceedings of the IEEE/CVF international conference on computer vision*,
 485 pp. 11975–11986, 2023.

486 Hangtao Zhang, Chenyu Zhu, Xianlong Wang, Ziqi Zhou, Changgan Yin, Minghui Li, Lulu Xue,
487 Yichen Wang, Shengshan Hu, Aishan Liu, et al. Badrobot: Jailbreaking embodied llms in the
488 physical world. *arXiv preprint arXiv:2407.20242*, 2024.

489 Xueyang Zhou, Guiyao Tie, Guowen Zhang, Hechang Wang, Pan Zhou, and Lichao Sun. Badvla:
490 Towards backdoor attacks on vision-language-action models via objective-decoupled optimiza-
491 tion. *arXiv preprint arXiv:2505.16640*, 2025.

492 Brianna Zitkovich, Tianhe Yu, Sichun Xu, Peng Xu, Ted Xiao, Fei Xia, Jialin Wu, Paul Wohlhart,
493 Stefan Welker, Ayzaan Wahid, et al. Rt-2: Vision-language-action models transfer web knowledge
494 to robotic control. In *Conference on Robot Learning*, pp. 2165–2183. PMLR, 2023.

495
496
497
498
499
500
501
502
503
504
505
506
507
508
509
510
511
512
513
514
515
516
517
518
519
520
521
522
523
524
525
526
527
528
529
530
531
532
533
534
535
536
537
538
539